materials

Review

An Overview of Recent Developments in Improving the Photocatalytic Activity of TiO_2-Based Materials for the Treatment of Indoor Air and Bacterial Inactivation

Achraf Amir Assadi [1,2], Oussama Baaloudj [3,4], Lotfi Khezami [5,*], Naoufel Ben Hamadi [5], Lotfi Mouni [6], Aymen Amine Assadi [7,*] and Achraf Ghorbal [2]

1 Center for Research on Microelectronics and Nanotechnology, CRMN Sousse Techno Park, Sahloul BP 334, Sousse 4054, Tunisia
2 Research Unit Advanced Materials, Applied Mechanics, Innovative Processes and Environment, Higher Institute of Applied Sciences and Technology of Gabes (ISSAT), University of Gabes, Gabes 6029, Tunisia
3 Laboratory of Reaction Engineering, Faculty of Mechanical Engineering and Process Engineering, Université des Sciences et de la Technologie Houari Boumediene, BP 32, Algiers 16111, Algeria
4 Laboratory of Advanced Materials for Energy and Environment, Université du Québec à Trois-Rivières (UQTR), 3351, Boul. des Forges, C.P. 500, Trois-Rivières, QC G9A 5H7, Canada
5 Chemistry Department, College of Science, Imam Mohammad Ibn Saud Islamic University (IMSIU), Riyadh 11432, Saudi Arabia
6 Laboratoire de Gestion et Valorisation des Ressources Naturelles et Assurance Qualité, Faculté SNVST, Université Bouira, Bouira 10000, Algeria
7 École Nationale Supérieure de Chimie de Rennes (ENSCR), Université de Rennes, UMR CNRS 6226, 11 Allée de Beaulieu, 35700 Rennes, France
* Correspondence: lhmkhezami@imamu.edu.sa (L.K.); aymen.assadi@ensc-rennes.fr (A.A.A.); Tel.: +966-11-2594-659 (L.K.); +33-(0)-223-238-152 (A.A.A.)

Citation: Assadi, A.A.; Baaloudj, O.; Khezami, L.; Ben Hamadi, N.; Mouni, L.; Assadi, A.A.; Ghorbal, A. An Overview of Recent Developments in Improving the Photocatalytic Activity of TiO_2-Based Materials for the Treatment of Indoor Air and Bacterial Inactivation. *Materials* **2023**, *16*, 2246. https://doi.org/10.3390/ma16062246

Academic Editors: Tongming Su and Xingwang Zhu

Received: 25 December 2022
Revised: 25 February 2023
Accepted: 27 February 2023
Published: 10 March 2023

Abstract: Indoor air quality has become a significant public health concern. The low cost and high efficiency of photocatalytic technology make it a natural choice for achieving deep air purification. Photocatalysis procedures have been widely investigated for environmental remediation, particularly for air treatment. Several semiconductors, such as TiO_2, have been used for photocatalytic purposes as catalysts, and they have earned a lot of interest in the last few years owing to their outstanding features. In this context, this review has collected and discussed recent studies on advances in improving the photocatalytic activity of TiO_2-based materials for indoor air treatment and bacterial inactivation. In addition, it has elucidated the properties of some widely used TiO_2-based catalysts and their advantages in the photocatalytic process as well as improved photocatalytic activity using doping and heterojunction techniques. Current publications about various combined catalysts have been summarized and reviewed to emphasize the significance of combining catalysts to increase air treatment efficiency. Besides, this paper summarized works that used these catalysts to remove volatile organic compounds (VOCs) and microorganisms. Moreover, the reaction mechanism has been described and summarized based on literature to comprehend further pollutant elimination and microorganism inactivation using photocatalysis. This review concludes with a general opinion and an outlook on potential future research topics, including viral disinfection and other hazardous gases.

Keywords: semiconductor; photocatalysis; indoor air treatment; volatile organic compounds; microorganism

1. Introduction

Air pollution and the degradation of air quality are becoming severe issues to deal with, but these notions often remain abstract and complex to surround or identify [1]. The contamination of food and drink raises a lot of interest since they are linked to vital daily elements for everyone [2]. Understanding how airborne particles can affect food and beverage quality is the first step to understanding how air filtration systems can address this issue [3]. Therefore, it is natural that the agri-food sector has a significant challenge in protecting its employees and processes against harmful atmospheric pollutants [4].

The primary pollutants confronted in indoor air include carbon monoxide (CO), microorganisms (fungi, bacteria, and viruses), nitrogen oxides (NOx), and a multitude of varieties of volatile organic compounds (VOCs) [5]. Given that in France, agri-food companies represent 15.3% of manufacturing industries with more than 17,647 companies [6], it is therefore essential and urgent to employ the purification system technology more effectively [7,8].

Numerous developing and encouraging technologies currently supply a solution to this issue [9,10]. Among them, heterogeneous photocatalysis in visible light proves its interest in compounds' degradation and/or mineralization [11,12]. However, these technologies do not make it possible to effectively guarantee constant purification over time of the microorganisms without the need for frequent maintenance operations due to their excessive bulk [13,14]. Advanced Oxidation Processes (AOPs) are processes that produce highly oxidizing species such as hydroxyl radicals ($^{\bullet}OH$) and other reactive oxygen species (ROS), including the anion superoxide radical ($^{\bullet}O_2^-$) and hydrogen peroxide (H_2O_2) capable of degrading target pollutants present in effluents [15,16]. The semiconductor material TiO_2 is considered a reference photocatalyst and an antibacterial agent due to its physicochemical properties [11,17,18]. However, TiO_2 has a wide bandgap, which limits its practical application in environmental remediation under visible light irradiation, including a wide range of the solar spectrum [16,19]. Many strategies have been implemented to overcome this concern, such as doping TiO_2 with metallic or non-metallic elements [20] and coupling with other semiconductors [21–23] to increase their absorption in the visible and improve the lifetime of electron-hole pairs [24]. It is possible to improve the redox process of pollutant degradation by doping TiO_2 with a metal oxide, which produces photoexcited charge carriers [25].

Indoor air quality has emerged as a significant public health problem. Photocatalytic technology is a natural solution for deep air filtration due to its low cost and excellent efficiency. Photocatalysis methods have been extensively researched for environmental remediation, notably for air treatment. Several semiconductors, such as TiO_2, have been used as photocatalytic catalysts, and they have gained a lot of attention in recent years due to their remarkable properties. For indoor air purification and bacterial inactivation, this review has compiled and evaluated current findings on improvements in the photocatalytic activity of TiO_2-based photocatalytic materials. The characteristics of various popular TiO_2-based catalysts and their benefits in the photocatalytic process have also been clarified, as well as how doping and heterojunction approaches might increase photocatalytic activity. Recent articles regarding diverse combined catalysts have been summarized and examined to underline the relevance of combining catalysts to boost efficiency. The studies that employ these catalysts to remove microorganisms and volatile organic compounds (VOCs) were also covered in this publication. Based on the literature, the reaction mechanism has also been defined and summarized to understand better pollutant removal and microorganism inactivation utilizing photocatalysis. Finally, this review's conclusion includes a summary and prognosis on prospective future study areas, such as viral disinfection and other dangerous gases. To our knowledge, there are few studies on the catalytic activity of alternative materials for indoor air treatment by eliminating both pollutants types, microorganisms, and VOCs.

2. Photocatalysis and Mass Transfer

Heterogeneous photocatalytic oxidation (HPO) is one of the active investigations in environmental treatment and purification [26–28]. It is widely applied in air pollution treatment, especially volatile organic compounds [29,30]. The resourceful technology is reserved for decomposing gaseous contaminants by employing photocatalysts under UV or solar light free of additional energy expenses [13,31].

2.1. Principle of Photocatalysis

Photocatalysis is generally described as the process of employing light (UV or visible light) to activate a substrate (such as a semiconductor photocatalyst) so that photo-reaction can be accelerated or facilitated with the catalyst remaining unconsumed [5]. The process can be divided into five steps (Figure 1):

(1) Transfer the reactants to the air phase.
(2) Adsorption of the reactants on the surface of the catalyst.
(3) Reaction in the adsorbed phase.
(3.1) Absorption of a photon by the catalyst.
(3.2) Generation of the electron-hole pairs.
(3.3) Separation of the pair.
(4) The oxidation and reduction with the adsorbed substrate.
(5) Desorption of the intermediate product.

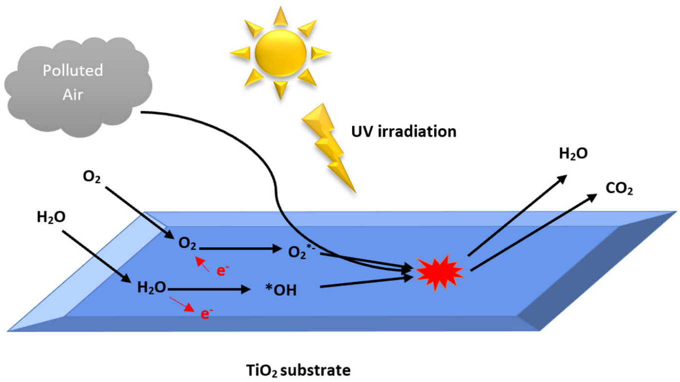

Figure 1. Polluted air photocatalysis treatment by TiO_2.

Among these five steps, the photocatalytic reaction is of crucial significance. It is initiated by the electron's excitation from the filled valence band (V_B) to the empty conduction band (C_B) of the photocatalyst when the energy carried by the absorbed photon equals or exceeds the band gap of the photocatalyst (Figure 2). In addition, the reaction results in the creation of a negative electron in the C_B and a positive hole in the V_B is called an electron-hole pair [32–34]. The positive hole oxidizes the hydroxide ion to yield hydroxyl radical ($^{\bullet}OH$), a potent oxidant of organic pollutants. The photo-excited electron is reduced to form the superoxide radical anion ($O_2^{\bullet-}$). These radicals are keys to the degradation of organic compounds [35].

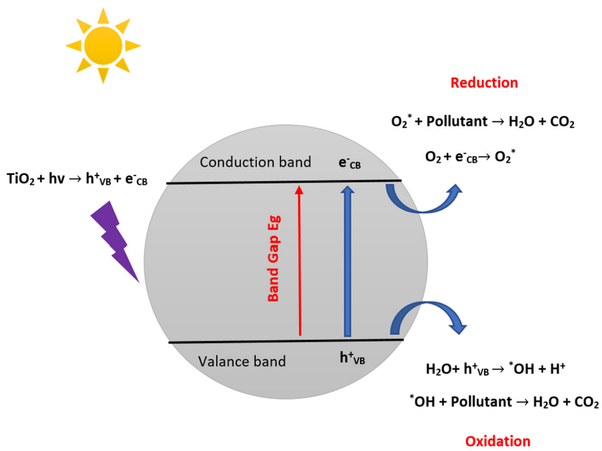

Figure 2. Schematic illustration of the photocatalytic reaction mechanism.

2.2. Development of Heterogeneous Photocatalytic Oxidation

Among all semiconductors, Titanium dioxide (TiO_2)-based materials have received particular attention in the photocatalysis field for their light absorption ability and high-efficiency treatment for both water and air; it was discovered by Fujishima and Honda in 1972 [36]. According to previous investigations, TiO_2-based photocatalysts also provide the advantages of high stability, availability, nontoxicity, excellent photoactivity, and low cost [35]. The photocatalysis of TiO_2 depends on variables such as specific surface area, crystallinity and surface hydroxyl groups of the TiO_2 [37]. This particular material has relatively polar surfaces that allow easy adsorption of hydrophilic pollutants. Nevertheless, titanium dioxide (TiO_2)-based materials have rapid recombination of electron-hole pairs, which, to some degree, suppresses the reaction efficiency [38,39].

Moreover, the band gap of materials is wide (3.0–3.2 eV), so the reaction is only activated with the irradiation of ultraviolet; hence the utilization of visible light irradiation is limited [14,40]. In order to improve the activity of photocatalysts under solar or artificial light at a lower energy cost and under more economic conditions, several strategies and investigations have been carried out to enhance the performance of TiO_2 [41]. These strategies include chemical modification, dye sensitization, and coupling with other semiconductor materials by introducing impurity atoms into pure TiO_2 to change electron-hole pairs concentrations in TiO_2 [35].

Metal doping is a method in which traces of foreign elements are introduced within the crystal lattice, and researchers widely use this strategy to reduce the band gap of titanium dioxide-based materials [42]. Noble metallic metals such as Ag, Au, Pt, and Pd have been researched extensively for years because of their properties and contribution to visible light absorption [5].

Ag is of particular interest as it acts as an electron trap and leads to retard the recombination of the electron-hole pair through the improvement of the transfer of interfacial charge [43]. Yi et al. studied a composite of Ag–AgI–TiO_2/CNFs; the Ag and I (Iodine) oxidation generated the reactive oxygen species (ROS) in the visible light range [44], doping TiO_2 with Ag and I increase its light range, increasing the photocatalytic activity. Yangfeng Chen et al. proposed a composite of heterostructured g-C_3N_4/Ag/TiO_2 microspheres by using the properties of Ag to delay the recombination of electron-hole pairs [45]. Apart from Ag, other metallic oxides can be composited with titanium dioxide to make the photo-reaction work under visible light. For example, halogens (X: Cl, Br, or I) bound to Bismuth oxide to form BiO_X, as a new class of promising catalyst has also drawn significant attention due to their attractive physicochemical characteristics, such as unique micro/nanostructures, bandgaps, optical and electrical properties and many other physicochemical characteristics [46–49]. Wendong Zhang et al. [49] found that the nanoplate BiOBr was highly efficient under visible light for NO photoreduction. Those promising catalysts (halogens) can be used as heterostructured photocatalysts with TiO_2 in order to enhance their photocatalytic activity. Actually, There is a lot of work done in heterogeneous photocatalysts with TiO_2, such as TiO_2/Ag [50], TiO_2/SiO_2 [51], TiO_2/Fe_2O_3 [52,53], TiO_2/Graphene [54] which have been shown to improve the photocatalytic performance of TiO_2, especially in the degradation of organic pollutants. These are only a few examples of TiO_2-based heterostructured photocatalysts. TiO_2 may be mixed with a variety of different substances to improve its photocatalytic activity. Aguilera-Ruiz also stated that cuprous oxide (Cu_2O), a visible-light-driven photocatalyst, has a band gap of about 2.07 eV [55]. Meanwhile, the conduction and valence band boundaries of $BiVO_4$ are located at 0.11 V and 2.65 V NHE. Thus, the composite Cu_2O/$BiVO_4$ has a promising photocatalytic performance under visible light [56]. Those two interesting materials, CuO and $BiVO_4$, can be used as the heterojunction or heterostructure to enhance the photocatalytic activity of the TiO_2-based catalysts. Moreover, it has been shown that Ag- V- and Fe-doped TiO2 achieved by various routes are very efficient in the oxidation of VOCs (butyl acetate, hexane or gaseous toluene) [57].

Non-metal doping is another strategy established to increase titanium dioxide's activity under solar or visible light. This technique takes advantage of the possible electronic transition from the induced new electronic states above TiO_2 V_B (2p or 3p orbitals of the dopant) to TiO_2 C_B (3d orbitals of Ti). Several researchers reported that the doped photocatalyst activity increases after non-metal doping, as the electronic structure has been modified to extend the absorption of the photocatalyst into the visible-light region [57]. Various studies have shown non-metal doping of TiO_2, such as Nitrogen-doped TiO_2 [58], carbon-doped TiO_2 [59–61], sulfur-doped TiO_2 [62,63], boron-doped TiO_2 [64] and phosphorus-doped TiO_2 [65]. Vaiano et al. studied recyclable visible-light active N-doped TiO_2 photocatalysts coated on glass spheres using a simple sol-gel method. They obtained excellent photocatalytic activity with visible light irradiation [66].

2.3. Reactors and Configurations

The configuration of reactors for air treatment is a critical element in the efficiency of the process. It should promote effective contact between the catalyst and the photons on the one hand and between the catalyst and the pollutants on the other. Care must also be taken to limit pressure drops. This part will present different continuous-flow photoreactors used in the laboratory or on an industrial scale.

Usually, this type of reactor is made up of a perforated plate placed at the inlet to ensure the homogeneity of the airflow. The central box contains two fixing devices for the photocatalytic support on one hand and a UV lamp on the other. In this configuration, the polluted air, driven by a fan, passes through the photocatalytic support. Another reactor configuration is based on using porous monolithic supports with varying thicknesses. The structure is based on the successive use of several UV lamps and monolithic "honeycomb" type photocatalytic media. The lamps irradiate the front and back sides of the monolithic supports.

The photocatalytic medium is placed against the reactor's internal wall and irradiated by a lamp set in a central tube. The particularity of this type of pilot is that the distance between the two plates or the diameters carrying the media is variable, which makes it possible to test the effect of the gap on the performance of the process.

Flat and cylindrical configurations:

A schematic representation of this rectangular configuration is used in the works of Assadi et his co-workers [3,5,17]. This reactor is formed by a chamber containing two glass plates at a variable distance. Each plate carries the photocatalytic media. Lamps are positioned along the length of the reactor at an equal distance in the inter-plate space [3,5,17].

The reactor is formed by two cylindrical tubes. The catalyst is installed on the inner wall of the outer cylinder. A UV lamp is installed in the inner tube in order to have uniform radiation from the catalytic surface. The gaseous effluent circulates between the outer tube's inner wall and the inner tube's outer wall. Note, To demonstrate the effect of material transfer, the diameter of the inner tube is studied to vary the thickness of the gas film [3,5,17].

Another planar configuration is based on surface-degraded fiber optic sheets on which titanium dioxide has been deposited. The latter replaced the bulky UV lamps. Optical fibers are used to activate the catalyst and further optimize the supply of UV radiation compared to lamps. This configuration will make it possible to inactivate the pollutants while offering compactness of the solution, i.e., lower pressure drops and easy handling in use. Figure 3 shows images of a fiber optic photocatalytic reactor and a fiber optic shee [3,5,17].

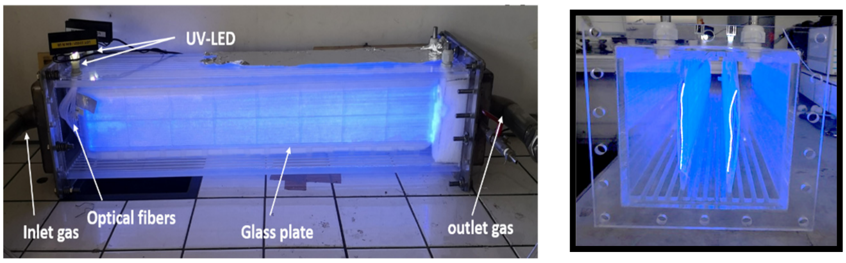

(**a**) (**b**)

Figure 3. (**a**) Images of a photocatalytic reactor based on optical fibers, (**b**) of a side view (Range of processed flow: from 5 at 20 m^3/h with concentrations varying from 5 to 50 mg/m^3) [5].

3. Volatile Organic Compounds (VOCs)

Volatile organic compounds are substances containing organic carbon which vaporize at significant rates [67,68]. They are the second-most widespread and various emissions classes after particulates [7]. Besides, we can state that as an approximate rule, VOCs are the organic liquids or solids whose vapor pressures at room temperature exceed 0.01 psi (=0.0007 atm) with atmospheric boiling points equal to or less than 480 °F estimated at 101.3 kPa, i.e., standard atmospheric pressure. Among hundreds of VOCs that have been qualitatively identified in the indoor environment, the main compounds are alkanes, alkenes, carboxylic acids and alcohols, esters, and aromatics [69]. Organic compounds are primarily found in home items such as wax, varnishes, and paints. All these chemicals can emit organic byproducts when utilized and stored in a non-controlled method. Studies have revealed that levels of numerous organic chemicals indoors are 2 to 5 times greater than outside. Therefore, with a specific level of time exposure, these organic compounds may have short or long term adverse health effects such as headaches, eye and respiratory tract irritation and even cancers [70].

VOCs in the atmosphere or the environment are relatively at low concentrations; hence, they are detectable based on interactions between the sensor component and the organic compounds. In addition, ventilation is also a conventional dilution method. Still, it is not firmly recommended in current practice because of its limitation on outdoor air quality (OAQ) and energy consumption [11,17,18]. Accordingly, researchers are still developing technologies and efficient approaches to meet IAQ standards and reduce energy costs to avail a secure, healthful, livable environment. During their research, Abidi and his collaborators studied the elimination of chloroform $CHCl_3$ by using different catalysts and analyzing the removal efficiency under several initial concentrations of each catalyst type supported on polyester under certain conditions [5]. Many works have demonstrated the ability of some TiO_2-based photocatalysts to remove VOCs from the air due to their high photocatalytic activity and stability [71]. Tobaldi et al., 2021 have reported that TiO_2-graphene oxide composites exhibit enhanced photocatalytic activity for the removal of various VOCs, such as benzene, toluene, and formaldehyde [72]. Another work has shown that TiO_2-carbon nanotube composite photocatalysts have efficient and improved photocatalytic activity for the removal of various VOCs, such as xylene and toluene [73]. The efficiency of the TiO_2 can be enhanced in its photocatalytic activity for the elimination of VOCs in the air by doping it with metal oxides such as ZnO, Fe_2O_3, and WO_3 [74], as this doping can increase the surface area and prevent electron-hole recombination. Table 1 summarizes several recent studies on the removal of VOCs using TiO_2-metal.

Table 1. List of some studies on using TiO_2-metal for VOCs removal.

Target Pollutants	Reactors	Catalyst	Radical Species	Operating Conditions	Degradation Performance	Formed Products (Intermediate and Final)	Ref.
Propionic acid (PPA) and benzene (BENZ)	annular reactor + dielectric barrier discharge (DBD)	SiO_2-TiO_2 + UV	°OH, CH_3 CH_2°	SiO_2 = 6.5 g m^{-2} et TiO_2 = 6.5 g m^{-2} performance lamp UV-A (80 W/10) output intensity (25 W/m^2) Odor inlet concentrations 0.068 to 0.405 mmol m^{-3}, Q = 2 at 6 m^3 h^{-1} relative Humidity: 5 to 90%, T = 20 °C	RE tested alone: 55% (APP) et 40% (BENZ) RE of mixture: 50% for APP and 30% for BENZ RE combined process: 60% for a voltage equal to 9 kV RE of mixture gaseous effluent (5% HR): 50% APP et 50% BENZ	BENZ: CO_2 dominating CO weak, O_3, CH_3CH_2OOH instable → Alcool + Aldéhyde → CO_2 PPA: CO_2, ethanoic acid (CH_3CH_2OOH), ethanol (CH_3CH_2OH), aldehyde (CH_3CHO), H_2O, O_2	[75]
Butane-2,3-dione and Heptane-2-one	Continuous Planar Reactor	TiO_2, TiO_2-Cu et TiO_2-Ag	•OH, O_2°−	Q = 1–12 m^3 h^{-1} concentration of COV= 5–20 mg.m^{-3} Humidity level = 5–70%, under UV-A light oxidation.	RE of TiO_2 alone: 63% RE of TiO_2-Ag: 46% RE of TiO_2-Cu: 52%	acetone (C_3H_5O) propionic acid ($C_3H_6O_2$) butanoic acid ($C_4H_8O_2$) pentanoic acid ($C_5H_{10}O_2$) acetic acid ($C_2H_4O_2$) acetaldehyde (C_2H_4O) formic acid (HCOH) carbon dioxide (CO_2) and H_2O	[76]
Acetone and toluene	Surface DBD discharge	Pt/TiO_2 and MnO2/CuO_2/Al_2O_3	NS	Concentration: 0.2 ppm flow rate: 38.42 m^3/h	100% toluene destruction of toluene at 0.2 ppm and 100% acetone destruction at 0.46 ppm	NS	[77]
Butane-2,3-dione (BUT) + *E. coli*	spherical batch reactor	Cu_2O/TiO_2 and TiO_2-Ag	•OH, HO_2° and O_2°−	Concentration: 4.4 g/m_3 T = 50 at 100 °C λ = 380–420 nm, under UV–vis light irradiation.	99.7% *E. coli* inactivation and 100% VOC degradation within 60 min and 25 min with TiO_2-Ag for simultaneous treatment	CO_2, H_2O	[78]

Table 1. *Cont.*

Target Pollutants	Reactors	Catalyst	Radical Species	Operating Conditions	Degradation Performance	Formed Products (Intermediate and Final)	Ref.
methyl ethyl ketone (MEK) or 2-butanone	annular reactor	TiO_2 (fiberglass + Ahlström support)	$^{\bullet}OH$, $O_2^{-\circ}$, $^{\circ}H_2C\text{-}CH_3$, $^{\circ}CH_3$, $H_3C\text{-}C^{\circ}{=}O$, $^{\circ}H_2C\text{-}CO\text{-}CH_2\text{-}CH_3$	MEK concentration on glass fibers: 1.51 mg/L MEK concentration on Ahlström: 1.75 mg/L HR glass fibers: 0.11–3.94 mW/cm^2 HR Ahlström: 0.12–2.53 mW/cm^2 T = 30 °C and 20 vol.% O_2, under UV light source.	Deposition of TiO_2 on glass fibers leads to 10% degradation of MEK for 1.5 mg/L. TiO_2 Ahlström leads to the elimination of 40% of MEK for 1.5 mg/L.	acetaldehyde (C_2H_4O) ethane (C_2H_6) methane (CH_4) methanol (CH_3OH) acetone (C_3H_6O) methyl formate ($C_2H_4O_2$) carbon dioxide (CO_2) and H_2O	[79]
Acetone	annular reactor	TiO_2 (fiberglass + Ahlström support)	$^{\circ}CH_3$, $^{\bullet}OH$, $H_2C^{\circ}\text{-}COOH$, $H_3C\text{-}^{\circ}C{=}O$	Concentration: 14.9 ng/L and 66.0 ng/L light power: 0.21 to 3.94 mW/cm^2 T = 30 °C, 20 vol.% O_2 Volume flow: 150 to 300 mL/min, under UV light.	90% of Acetone conversion has been obtained for low initial concentrations with TiO_2 photocatalyst deposited on fiberglass for simultaneous treatment	acetaldehyde (C_2H_4O) methyl alcohol (CH_3OH) isopropyl alcohol (C_3H_8O) methyl ethyl ketone (C_4H_8O) acetic acid (CH3 COOH) mesityl oxide ($C_6H_{10}O$) diacetone-alcohol ($C_6H_{12}O_2$)	[80]
Benzene	the outer surface of the rectangular SiC ceramic membrane	$Pt/SiC@Al_2O_3$	NS	0.176% by mass of Pt	90% reduction at 215 °C with a space velocity of 6000 mg^{-1} h^{-1}	CO_2, H_2O	[81]
n-butanol and acetic acid	fixed-bed tubular reactor	$Pt/CeO_2\text{-}AlO_3$	NS	1000 ppm of COV T = 50–350 °C 0, 7, 15, 23 et 51% by weight of CeO_2	100% reduction for n-butanol at T < 250 °C 50 or 90% reduction for a reduction of 80 or 20 °C.	Butanal (C_4H_8O) methanol (CH_4OH) propanol (C_3H_8O) isopropanol (C_3H_8O) formaldehyde (HCOH) propanal (C_3H_6O) carbon dioxide (CO_2)	[82]

Table 1. *Cont.*

Target Pollutants	Reactors	Catalyst	Radical Species	Operating Conditions	Degradation Performance	Formed Products (Intermediate and Final)	Ref.
Formaldehyde	organic glass reactor	Pt/AlOOH/, Pt/AlOOH-c, Pt/c-Al_2O_3 and Pt/TiO_2	NS	HCHO concentration: 127 ppm for adsorption and 139 ppm for catalytic oxidation, fan: 5 W T: 35 °C HR: 25% oxidation time: 51 min.	Pt/AlOOH > Pt/AlOOH-c > Pt/c-Al_2O_3 > Pt/TiO_2	surface formate carbon dioxide (CO_2) water (H_2O)	[83]
Formaldehyde	fixed-bed quartz flow reactor	Ag/TiO_2, Ag/Al_2O_3 et Ag/CeO_2	NS	Concentration: 110 ppm T = 35 to 125 °C Debit: 100 mL min^{-1}, under light containing ultraviolet.	Ag/TiO_2 > Ag/Al_2O_3 > Ag/CeO_2 100% HCHO conversion with Ag/TiO_2 at T = 95°C	carbon dioxide (CO_2) another carbon-containing compound	[84]
Formaldehyde	NS	Pt/TiO_2, Rh/TiO_2, Pd/TiO_2, Au/TiO_2 (noble metals/TiO_2)	NS	Concentration: 100 ppm 1% noble metals/TiO_2 O_2 20 vol.% Debit: 50 cm^3 min^{-1} T: 20 °C GHSV: 5000 h^{-1}	Pt/TiO_2 ≫ Rh/TiO_2 > Pd/TiO_2 > Au/TiO_2	carbon dioxide (CO_2)carbon monoxyde (CO); water (H_2O)	[85]
Dimethyl disulfide (DMDS)	Continuous Flow Quartz Tubular Reactor	(Au + Pd)/TiO_2, Au/MCM-41, (AU + Rh)/MCM and Au/TiO_2, Pd/TiO_2	NS	3%Pd/TiO_2 and 1%Au/TiO_2(1%Au + 3%Pd)/TiO_2 gas flow: 42,000 h^{-1} Temperature: 20–320 °C	Au/TiO_2 and Au-Pd/TiO_2 effectively remove DMDS for T < 155 °C Au/MCM-41 less effective in DMDS eliminating	methanol (CH_3OH) ethanol (C_2H_6O) methyl mercaptan (CH_3SH) ethyl mercaptan (CH_3SCH_3) hydrogen sulfur (H_2S) carbon dioxide (CO_2) carbon monoxide (CO) sulfur dioxide (SO_2) water (H_2O)	[86]

Table 1. *Cont.*

Target Pollutants	Reactors	Catalyst	Radical Species	Operating Conditions	Degradation Performance	Formed Products (Intermediate and Final)	Ref.
toluene + m-xylene + ethyl acetate or acetone	fixed-bed Quartz Continuous Flow Microreactor (ICP-AES)	0.91 wt.% $Au_{0\cdot48}$ Pd/α-MnO_2et α-MnO_2	α-, β- et γ-oxygène	1% (Au-Pd) Mixing flow: 17 mL/min concentration: 1000 ppm + O_2 + N_2 (solid) molar ratio COV/O_2 = 1/400 SV (space velocity) = 40,000 mL (g h) T = 320 °C	0.91 wt.% Au 0.48 Pd/α-MnO_2 > α-MnO_2	carbon dioxide (CO_2)water (H_2O)	[69]
Isovaleraldehyde	continuous annular plasma reactor DBD combined photocatalysis	TiO_2	$^{\bullet}OH$, $O_2^{\bullet-}$	concentration: 75 to 200 mg m^{-3} Debit: 2 m^3 h^{-1} HR: 5% T: 20 °C I: 20 W m^{-2} SE: 17 J L^{-1}, under UV light.	NS	propanoic acid (CH_3CH_2COOH) propanone (CH_3COCH_3) ethanoic acid (CH_3COOH) carbon dioxide (CO_2) carbon monoxide (CO) ozone (O_3)	[87]
Benzene	New UV-LED frontal flow photocatalytic reactor	TiO_2 deposed on luminous textiles	OH°, $O_2^{\circ-}$	concentration: 100 to 200 mg m^{-3} Debit: 1 m^3 h^{-1} HR: 5 to 80% T: 20 °C		CO_2 and H_2O	[72]

4. Microorganism Inactivation and Reactional Mechanisms

Understanding the mechanism of the bactericidal effect action of semiconductors is fundamental to improving its activity and, in particular, involves the analysis of the targets of TiO_2 at the bacterial level [88]. TiO_2 is a multifunctional photocatalyst that may be utilized to render microorganisms inactive [61]. The following steps are involved in the overall process for the inactivation of microorganisms using TiO_2. Step 1: TiO_2 is exposed to irradiation and undergoes a photocatalytic reaction that produces ROS like hydroxyl radicals (*OH) and superoxide radicals ($O_2{*}^{-}$). Step 2: ROS is formed in the photocatalytic reaction and interacts with bacterial cells and membranes and damaging DNA, proteins, and lipids. In addition, ROS can combine with water molecules to form more ROS, such as H_2O_2. Damages and harm caused by ROS interactions lead then to step 3 inactivation of the microorganism, in which the cell of the microorganism dies. The general microorganisms' photocatalytic inactivation mechanisms of TiO_2 can be summarized by the following equations and Figure 4:

$$TiO_2 + hv \rightarrow TiO_2\ (C_B\ e^-) + TiO_2\ (V_B\ h^+) \quad (1)$$

$$O_2 + e^- \rightarrow O_2{}^{-*} \quad (2)$$

$$H_2O + h^+ \rightarrow H^+ + {}^*OH \quad (3)$$

$${}^*OH + O_2{}^{-*} + \text{Microorganism} \rightarrow \text{Inactivated Microorganism} \quad (4)$$

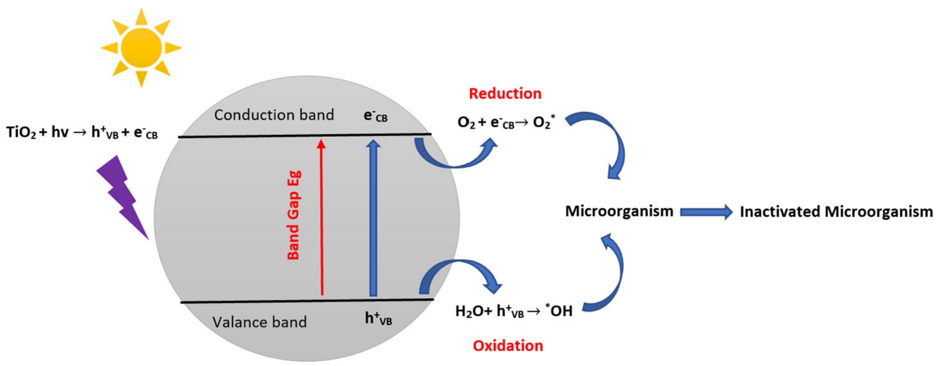

Figure 4. Schematic illustration of the antibacterial photocatalytic mechanisms of TiO_2 (inspired from ref. [89]).

Overall, because TiO_2 is ecologically neutral and doesn't produce toxic byproducts, using it as a photocatalyst to inactivate bacteria presents a viable substitute for conventional disinfection techniques that involve chemicals or heat [90]. The effectiveness of TiO_2-based photocatalysis, however, is dependent on several variables, including the characteristics of the TiO_2, the strength and wavelength of the light source, and the kind and quantity of bacteria present [91]. The inorganic semiconductors doping or adding a co-catalyst, such as TiO_2, with metals such as Cu, mainly accelerates bacterial inactivation kinetics [76,92]. Different reactions will likely be generated when the copper oxides are in contact with the catalyst's surface [76,92]. Indeed, CuO and Cu_2O are spawned when there is an interaction between copper and O_2 (air) under light irradiation. Cu_xO is found in two forms (CuO and Cu_2O) and exhibits the Cu(+I) and Cu(+II) oxidation states, of which the main form that interacts with bacteria and VOCs is Cu_2O, thus generating electrons at the level of the conduction band; Cu_2O ($C_B\ e^-$) and holes in the valence band; Cu_2O ($V_B\ h^+$) [78,92,93]. Under simulated sunlight, Cu_2O ($C_B\ e^-$) enters a reduction reaction with TiO_2 to reduce Ti^{4+} to Ti^{3+} and yields Cu(+I) at the $V_B\ h^+$ level, which may lead to bacterial inactivation and/or VOCs to form CO_2, H_2O, N, S and inactivated bacteria [17,76,92]. The main antibacterial photocatalytic mechanisms of TiO_2 with Cu_2O suggested by previous research papers cited above can be summarized by the following equations and Figure 5 [78,92,93]:

$$Cu_2O + hv \rightarrow Cu_2O\ (C_B\ e^-) + Cu_2O\ (V_B\ h^+) \quad (5)$$

$$Cu_2O\ (C_B\ e^-) + TiO_2 \rightarrow TiO_2^-\ \text{ou}\ (Ti^{3+}) + Cu_2O \quad (6)$$

$$TiO_2^- + O_2 \rightarrow TiO_2 + O_2^{-*} \quad (7)$$

$$^\circ O_2^- + h^+ \rightarrow H_2O^* \quad (8)$$

$$H_2O^* + h^+ + e^-_{cb} \rightarrow H_2O_2 \quad (9)$$

$$H_2O_2 + e^-_{cb} \rightarrow OH + {}^*OH \quad (10)$$

$$Cu_2O\ (V_B\ h^+) + \text{bacteria} \rightarrow CO_2\ \text{and}\ H_2O \quad (11)$$

$$h^+ + \text{Bacteria} \rightarrow \text{Inactivated Bacteria} \quad (12)$$

$$H_2O_2 + \text{Bacteria} \rightarrow \text{Inactivated Bacteria} \quad (13)$$

$$^*OH + \text{Bacteria} \rightarrow \text{Inactivated Bacteria} \quad (14)$$

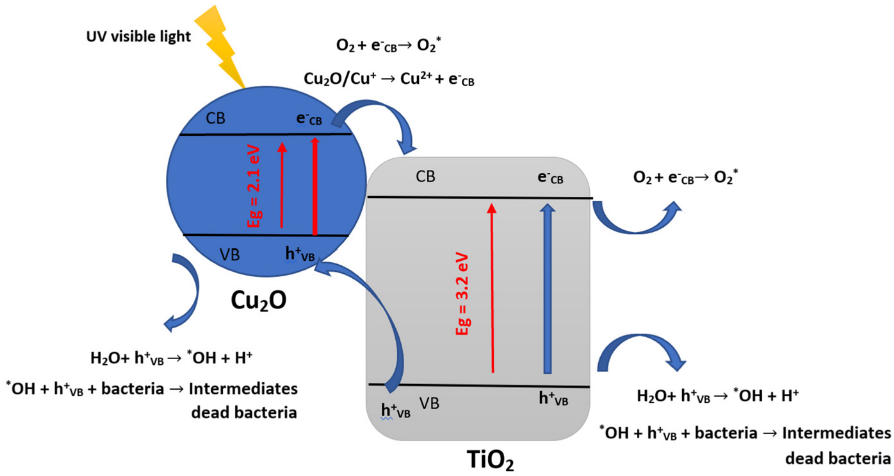

Figure 5. The main antibacterial photocatalytic mechanisms of TiO_2 with Cu_2O (inspired from refs. [78,92,93]).

The inactivation of bacteria cells can occur by many processes during the photocatalytic reactions, either the rupture of the cell membrane (Membrane disruption), the cell wall (Exposed cellular components), or the attack of the cells by ROS [19]. Where high levels of oxidative stress may be produced by ROS, which interacts with bacterial cells effectively and kills them by destroying the cell wall and a variety of bacterial cell components such as protein, lipids, carbohydrates, DNA, and amino acids [94]. Furthermore, when photocatalyst particles are deposited at the surface of bacterial cells, they can interact with them via diffusion and endocytosis mechanisms, which induce the destruction of membrane proteins or cell membranes owing to the phenomena of member permeability [19]. Moreover, both catalysts and generated ROS can interfere with the movement of electrons within the cell microorganisms, loss of protein motive force, depletion of intracellular ATP production with DNA replication disintegration, and intracellular outflow resulting in bacteria cell inactivation [95].

The hydroxyl radicals (*OH) produced on the surface of copper (Cu^+) in contact with H_2O with the holes generated at the level of $V_B\ h^+$ is the primary ROS involved in bacterial inactivation [29,96]. Cu_2O exhibits high bacterial inactivation capacity when light irradiation stimulates electron transfer between copper and bacterial cells and produces reactive oxygen species (ROS), resulting in bacterial cell inactivation [78,97,98]. Abidi et al.

investigated the effects of Cu_xO amounts at different sputtering times on the TiO_2-Polyester (PES) photocatalyst in the inactivation of microorganisms [17]. For sputtering intensities ranging from 20 to 80 A, it was regarded that the Cu_xO/TiO_2–PES catalyst sputtered at 80 A; the total inactivation of the bacteria was obtained after an hour of exposure to indoor light. Copper oxide showed high antibacterial activity, and the intrinsic activity of Cu(+I) can be enhanced by UV-vis illumination [17].

Additionally, Ag-NP is an excellent material used to improve the photocatalytic inactivation of microorganisms using TiO_2, which has recently been proven in previous works [76]. Ag particles could inactivate bacteria as Ag-NP is an essential factor that controls and regulates antimicrobial activity [92].On contact of Ag with TiO_2 under light irradiation, either Ag(0), Ag(+I), or Ag(+II) are yielded. The release of these different forms of Ag in contact with *Escherichia coli* induces bacterial inactivation [99]. The Ag used for TiO_2-NT decoration showed +1 and +2 oxidation states (Ag^+ and Ag^{2+}) [78].

In its metallic state, silver is oxidized in the air (O_2), breeding Ag_2O; this substance yields Ag^+ ions. This 4-electron process can be outlined by the following two equations [99]:

$$4\ Ag^0 + O_2 \rightarrow 2\ Ag_2O \tag{15}$$

$$2\ Ag_2O + 4H^+ \rightarrow 4\ Ag^+ + 2\ H_2O \tag{16}$$

Ag_2O is at the origin of the inactivation of bacteria when it generates the production of reactive oxygen species in contact with TiO_2-NTs. While Ag_2O is in contact with TiO_2 as a semiconductor, electrons (e^-) are photo-generated by the semiconductor under the action of bandgap radiation as indicated by the chemical reaction (Equation (20)) and photo-generated holes (h^+) react with H_2O (Equation (18)) to yield hydroxyl radicals (OH°) [76,92]:

$$Ag_2O + e^- \rightarrow 2\ Ag^+ + \frac{1}{2}\ O_2{}^- \tag{17}$$

$$h^+ + H_2O \rightarrow {}^*OH + H^+ \tag{18}$$

$$2H_2O + O_2 + 2e^- \rightarrow 2\ {}^*OH + 2\ OH^- \tag{19}$$

$$e^- + O_2 \rightarrow O_2{}^{*-} \tag{20}$$

The suggested bacterial inactivation mechanism with Ag/TiO_2 under light can be recapitulated in the following equations [76] and Figure 6:

$$Ag_2O + hv \rightarrow Ag_2O\ (C_B\ e^-) + Ag_2O\ (V_B\ h^+) \tag{21}$$

$$Ag_2O\ (e^- + h^+) + TiO_2 \rightarrow Ag_2O\ (V_B\ h^+) + TiO_2\ (C_B\ e^-) \tag{22}$$

$$TiO_2\ (C_B\ e^-) + O_2 \rightarrow TiO_2 + O_2 \tag{23}$$

$$2\ e^- + O_2 + 2H^+ \rightarrow H_2O_2 \tag{24}$$

$$H_2O_2 + O_2{}^- \rightarrow {}^*OH + OH^- + O_2 \tag{25}$$

$$Ag_2O\ (V_B\ h^+) + \text{Bacteria} \rightarrow \text{Inactivated Bacteria} \tag{26}$$

$$H_2O_2 + \text{Bacteria} \rightarrow \text{Inactivated Bacteria} \tag{27}$$

$$ {}^*OH + \text{Bacteria} \rightarrow \text{Inactivated Bacteria} \tag{28}$$

$$ {}^*OH + \text{VOCs} \rightarrow CO_2 + H_2O \tag{29}$$

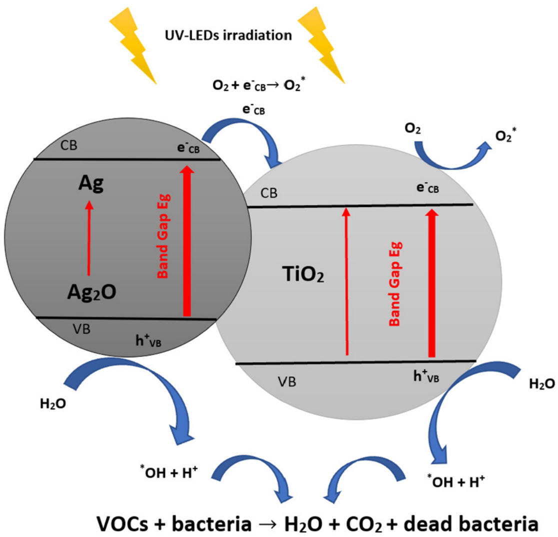

Figure 6. The main antibacterial photocatalytic mechanisms of TiO_2 with Ag_2O (inspired from ref [76]).

It is well known that the reaction of oxygen radicals in the cell causes its death [96]. Furthermore, different bacteria have different membrane structures [100]. For example, Gram − bacteria have peptidoglycan of the wall less thick than Gram + bacteria, which have an additional outer membrane composed of a double layer of lipids. This finding is in chains of different catalytic reactions and further disinfection efficiencies [101]. Accordingly, other bacteria's survival rates will differ under identical disinfection conditions [102].

The most critical mechanism in antibacterial activity is cell membrane damage. Oxidative stress generated by ROS is a second mechanism involved in antibacterial activity [103–105]. This stress inhibits DNA replication, protein synthesis, and cellular metabolism, causing cell death [106]. In order to demonstrate the effect of ROS on cell death, a study was conducted in the absence and presence of L-cysteine, a natural antioxidant, with *E. coli* bacteria. Indeed, growth was inhibited by Cu-TiO_2/GF with an efficiency of 79.4% in the absence of L-Cysteine compared to 65.1% in its presence. Similarly, Ag-TiO_2/GF, where the efficiency was 100% without the antioxidant and diminished to 84.7% in its presence [92]. The experiment is conducted on the following bacteria: *E. coli* and *Staphylococcus aureus* (*S. aureus*) on copper-doped TiO_2/GF and silver-doped TiO_2/GF synthesized by sol-gel method, and at different relative humidities (Table 2).

Overall, silver-doped TiO_2/GF performed best on both bacteria, followed closely by copper TiO_2/GF and [107] then TiO_2/GF alone. The yield was better at a relative humidity of 60% than 80%. They were significantly lower at 40% humidity. *E. coli* is eliminated reasonably than *S. aureus* since the latter is a Gram + bacterium with a more complex wall [76,92].

Table 2. List of some studies on using TiO_2-metal for bacterial inactivation.

Bio Contaminants	Reactor	Catalyst	Operations Parameters	Performance	Ref.
E. coli	Petri dishes	TiO_2-NT and Ag-TiO_2-NTs	Concentration: 4 × 10^6 UFC/mL volume: 100 mL diameter TiO_2: 100 nm at 70V diameter Ag: 8 nm	TiO_2: reduction of 1.6 log with 180 min Ag/TiO_2: reduction of 99.99% after 90 min	[107]
P. aeruginosa	Glass fiber tissue (GFT)	Poroux $TiO_2$$TiO_2$ pur (TiO_2-PEG) and TiO_2-Ag	Concentration: 10^3 UFC/mL TiO_2 pur: 14.7 nm TiO_2-Ag-PEG:16.6 nm TiO_2-Ag: 25.3 nm, under UV light.	TiO_2-1Ag: 100% of inactivation after 10 min TiO_2 poroux: 57% TiO_2-PEG: 93%	[108]
E. coli K12	Agar matrix surface + blueberry skin + calyx	UV-TiO_2& UV alone	Initial bacterial populations: 7 log CFU/g UV-Photocatalysis (4.5 mW/cm^2) UV alone (6.0 mW/cm^2). TiO_2-coated quartz tubes (38 cm length, 24.5 mm outer diameter, thickness 0.7–0.9 mm.	4.5 log CFU/g for UV alone and 5.3 log CFU/g for UV-TiO_2 in 30 s. 3.4 log and 4.6 log CFU/g, respectively, UV alone and UV-TiO_2 for the first 30 s. 4.0 log and 5.2 log CFU/g, respectively, UV alone and photocatalysis.	[109]
S. aureus. P. aeruginosa and *E. coli*	LB agar plates	TiO_2-Ag (TiO_2 (calcinated at 300 °C) (CB300) at (500 °C$_)$ (CB500) et TiO_2 (not calcinated) (CB))	Concentration: 10 µL with 10^9 UFC/mL 5%w of TiO_2	TiO_2 (calcined 300 °C)-Ag: reduces bacterial growth by 95%, i.e., 1.05 × 10^8 CFU/mL with UV. TiO_2 (calcined 500 °C) without Ag: reduces bacterial growth by 30% with UV. TiO_2 (calcined at 300 °C) without Ag: reduces growth by 75%.	[110]
E. coli	Planar reactor	TiO_2, TiO_2-Ag and TiO_2-Cu deposed on optical fibers	Initial bacterial populations: 2.4 × 10^7 UFC/mL. The core of optical fibers is constructed of polymethyl methacrylate resin with a mean diameter of 480 m and coated with 10 m of a thick fluorinated polymer, under UVA-LEDs (365 nm, UVA-LED intensity = 1.5 W m^{-2}).	3 log of removal with TiO_2/Ag and TiO_2/Cu	[76]

Table 2. *Cont.*

Bio Contaminants	Reactor	Catalyst	Operations Parameters	Performance	Ref.
S. aureus CCM 3955 & *S. aureus* CCM 3953 (Gram+) *E. coli* & *P. aeruginosa* (Gram−)	Disposable plates	Ag NPs	Initial bacterial populations: from 10^5 to 10^6 UFC/mL, Particle size from 40 to 60 nm, Temperature 35 °C.	Higher activity at 7 ppm against *P. aeruginosa*. NP Ag synthesized based on $AgNO_3$: considerable antibacterial activity at 14 and 29 ppm (82.49% inactivation). NP Ag synthesized based on $AgNO_3$ and citrate: 88.56 inactivations.	[111]
E. coli	Batch reactor	Cu_2O-NPs/TiO_2-NTs catalyst	Initial bacterial populations: from 10^6 to 10^7 UFC/mL. Under visible light irradiation (380–720) nm. Temperature 37 °C.	Bacterial inactivation rate of 98% and a concomitant 99.7% VOC removal within 60 min and 25 min	[78]

5. Conclusions and Outlook

Recent studies on photocatalysis for indoor air purification and bacterial inactivation have shown promising results. Even though a variety of photocatalysts are available, TiO_2-based materials are the most effective or, at the very least, effective option for practical and financial reasons. This review has collected and covered recent research that has improved the photocatalytic activity of materials based on TiO_2 for VOC degradation in indoor air and bacterial inactivation. Coupling TiO_2 materials with other methods has been increasingly explored. This paper also reviewed the literature on the material aspects of photocatalysis based on AgxO/TiO_2 and CuxO/TiO_2 to treat air-containing chemical and biological pollution. A bibliographical synthesis of the type of catalyst and the operating conditions was detailed concerning the decontamination of VOCs. Moreover, the different types of microorganisms treated by TiO_2-based photocatalysts have been listed. In-depth explanations of the reaction mechanisms for photocatalytic degradation and inactivation have been provided. As a look ahead to future research, we believe more study and testing are needed to clarify and comprehend the benefits of TiO_2-based materials on photocatalytic applications. There are only a few works on the combined treatment of chemical and biological pollution using photocatalysis at the same time. The investigations do not consider evaluating removal or if mineralization is complete, which is an essential criterion because it can generate more harmful intermediates than the pollutant. Finally, experiments in real cases of air pollution, such as hospital air pollution, are required to apply this process.

Author Contributions: Conceptualization, A.A.A. (Achraf Amir Assadi) and O.B.: methodology and writing—review, A.A.A. (Achraf Amir Assadi), N.B.H., L.K. and A.A.A. (Aymen Amine Assadi); writing—review and editing, A.A.A. (Achraf Amir Assadi), A.A.A. (Aymen Amine Assadi) and L.M.; conceptualization, funding acquisition, L.M.; methodology, L.K.; resources, project administration, supervision, A.A.A. (Aymen Amine Assadi): writing-review and editing, A.G. and L.M. All authors have read and agreed to the published version of the manuscript.

Funding: This research received no external funding.

Institutional Review Board Statement: Not applicable.

Informed Consent Statement: Not applicable.

Acknowledgments: The authors extend their appreciation to the Deanship of Scientific Research at Imam Mohammad Ibn Saud Islamic University (IMSIU) for funding and supporting this work through Research Partnership Program no RP-21-09-66.

Conflicts of Interest: The authors declare no conflict of interest.

References

1. Cincinelli, A.; Martellini, T. Indoor air quality and health. *Int. J. Environ. Res. Public Health* **2017**, *14*, 1286. [CrossRef]
2. Capolongo, S.; Settimo, G.; Gola, M. (Eds.) *Indoor Air Quality (IAQ) in Healthcare Facilities*; Springer: Berlin/Heidelberg, Germany, 2017; Volume 4386.
3. Assadi, I.; Guesmi, A.; Baaloudj, O.; Zeghioud, H.; Elfalleh, W.; Benhammadi, N. Review on inactivation of airborne viruses using non-thermal plasma technologies: From MS_2 to coronavirus. *Environ. Sci. Pollut. Res.* **2021**, *29*, 4880–4892. [CrossRef]
4. Heinsohn, R.J.; John, M.C. (Eds.) *Indoor Air Quality Engineering: Enviromental Health and Control Indoor*; CRC Press: Boca Raton, FL, USA, 2003; ISBN 0-8247-4061-0.
5. Abidi, M.; Hajjaji, A.; Bouzaza, A.; Lamaa, L.; Peruchon, L.; Brochier, C.; Rtimi, S.; Wolbert, D.; Bessais, B.; Assadi, A.A. Modeling of indoor air treatment using an innovative photocatalytic luminous textile: Reactor compactness and mass transfer enhancement. *Chem. Eng. J.* **2022**, *430*, 132636. [CrossRef]
6. Salmon, D.G. Annual Exporter Guide France. Available online: https://www.google.com.hk/url?sa=i&rct=j&q=&esrc=s&source=web&cd=&ved=0CAQQw7AJahcKEwjw49TzpND9AhUAAAAAHQAAAAAQAg&url=https%3A%2F%2Fapps.fas.usda.gov%2Fnewgainapi%2Fapi%2Freport%2Fdownloadreportbyfilename%3Ffilename%3DExporter%2520Guide_Paris_France_12-8-2014.pdf&psig=AOvVaw0bBETSpKjn6_G28dOcdT4j&ust=1678500724709337 (accessed on 25 December 2022).
7. Erisman, J.W. Air Pollution Science for the 21st Century. *Environ. Sci. Policy* **2003**, *6*, 396. [CrossRef]

8. Quyen, N.T.; Traikool, T.; Nitisoravut, R.; Onjun, T. Improvement of water quality using dielectric barrier discharge plasma. *J. Phys. Conf. Ser.* **2017**, *860*, 12031. [CrossRef]
9. Pichat, P. Some views about indoor air photocatalytic treatment using TiO_2: Conceptualization of humidity effects, active oxygen species, problem of C1-C3 carbonyl pollutants. *Appl. Catal. B Environ.* **2010**, *99*, 428–434. [CrossRef]
10. Ghezzi, S.; Pagani, I.; Poli, G.; Perboni, S.; Vicenzi, E. Rapid Inactivation of Severe Acute Respiratory Syndrome Coronavirus 2 (SARS-CoV-2) by Tungsten Trioxide-Based (WO_3) Photocatalysis. *bioRxiv* **2020**. [CrossRef]
11. Assadi, A.A.; Karoui, S.; Trabelsi, K.; Hajjaji, A.; Elfalleh, W.; Ghorbal, A.; Maghzaoui, M.; Assadi, A.A. Synthesis and Characterization of TiO2 Nanotubes (TiO2-NTs) with Ag Silver Nanoparticles (Ag-NPs): Photocatalytic Performance for Wastewater Treatment under Visible Light. *Materials* **2022**, *15*, 1463. [CrossRef]
12. Malayeri, M.; Haghighat, F.; Lee, C.S. Kinetic modeling of the photocatalytic degradation of methyl ethyl ketone in air for a continuous-flow reactor. *Chem. Eng. J.* **2021**, *404*, 126602. [CrossRef]
13. Zhang, Z.; Gamage, J. Applications of photocatalytic disinfection. *Int. J. Photoenergy* **2010**, *2010*, 764870. [CrossRef]
14. Bono, N.; Ponti, F.; Punta, C.; Candiani, G. Effect of UV irradiation and TiO_2-photocatalysis on airborne bacteria and viruses: An overview. *Materials* **2021**, *14*, 1075. [CrossRef] [PubMed]
15. Ali, I.; Al-hammadi, S.A.; Saleh, T.A. Simultaneous sorption ofdyes and toxic metals from waters using synthesized titania-incorporated polyamide. *J. Mol. Liq.* **2018**, *269*, 564–571. [CrossRef]
16. Ali, T.; Ahmed, A.; Alam, U.; Uddin, I.; Tripathi, P.; Muneer, M. Enhanced photocatalytic and antibacterial activities of Ag-doped TiO_2 nanoparticles under visible light. *Mater. Chem. Phys.* **2018**, *212*, 325–335. [CrossRef]
17. Abidi, M.; Assadi, A.A.; Bouzaza, A.; Hajjaji, A.; Bessais, B.; Rtimi, S. Photocatalytic indoor/outdoor air treatment and bacterial inactivation on CuxO/TiO_2 prepared by HiPIMS on polyester cloth under low intensity visible light. *Appl. Catal. B Environ.* **2019**, *259*, 118074. [CrossRef]
18. Zhang, Y.; Zhao, X.; Fu, S.; Lv, X.; He, Q.; Li, Y.; Ji, F.; Xu, X. Preparation and antibacterial activity of Ag/TiO_2-functionalized ceramic tiles. *Ceram. Int.* **2022**, *48*, 4897–4903. [CrossRef]
19. Baaloudj, O.; Assadi, I.; Nasrallah, N.; El, A.; Khezami, L. Simultaneous removal of antibiotics and inactivation of antibiotic-resistant bacteria by photocatalysis: A review. *J. Water Process Eng.* **2021**, *42*, 102089. [CrossRef]
20. Wu, Y.; Chen, X.; Cao, J.; Zhu, Y.; Yuan, W.; Hu, Z.; Ao, Z.; Brudvig, G.W.; Tian, F.; Yu, J.C.; et al. Photocatalytically recovering hydrogen energy from wastewater treatment using MoS_2@TiO_2 with sulfur/oxygen dual-defect. *Appl. Catal. B Environ.* **2022**, *303*, 120878. [CrossRef]
21. Assadi, A.A.; Bouzaza, A.; Wolbert, D. Study of synergetic effect by surface discharge plasma/TiO_2 combination for indoor air treatment: Sequential and continuous configurations at pilot scale. *J. Photochem. Photobiol. A Chem.* **2015**, *310*, 148–154. [CrossRef]
22. Karoui, S.; Ben Arfi, R.; Mougin, K.; Ghorbal, A.; Assadi, A.A.; Amrane, A. Synthesis of novel biocomposite powder for simultaneous removal of hazardous ciprofloxacin and methylene blue: Central composite design, kinetic and isotherm studies using Brouers-Sotolongo family models. *J. Hazard. Mater.* **2020**, *387*, 121675. [CrossRef]
23. Zeghioud, H.; Khellaf, N.; Amrane, A.; Djelal, H.; Elfalleh, W.; Assadi, A.A.; Rtimi, S. Photocatalytic performance of TiO_2 impregnated polyester for the degradation of Reactive Green 12: Implications of the surface pretreatment and the microstructure. *J. Photochem. Photobiol. A Chem.* **2017**, *346*, 493–501. [CrossRef]
24. Baaloudj, O.; Kenfoud, H.; Badawi, A.K.; Assadi, A.A.; El Jery, A.; Assadi, A.A.; Amrane, A. Bismuth Sillenite Crystals as Recent Photocatalysts for Water Treatment and Energy Generation: A Critical Review. *Catalysts* **2022**, *12*, 500. [CrossRef]
25. Kappadan, S.; Gebreab, T.W.; Thomas, S.; Kalarikkal, N. Tetragonal BaTiO3 nanoparticles: An efficient photocatalyst for the degradation of organic pollutants. *Mater. Sci. Semicond. Process.* **2016**, *51*, 42–47. [CrossRef]
26. Malato, S.; Fernández-Ibáñez, P.; Maldonado, M.I.; Blanco, J.; Gernjak, W. Decontamination and disinfection of water by solar photocatalysis: Recent overview and trends. *Catal. Today* **2009**, *147*, 1–59. [CrossRef]
27. Koe, W.S.; Lee, J.W.; Chong, W.C.; Pang, Y.L.; Sim, L.C. An overview of photocatalytic degradation: Photocatalysts, mechanisms, and development of photocatalytic membrane. *Environ. Sci. Pollut. Res.* **2020**, *27*, 2522–2565. [CrossRef]
28. Akerdi, A.G.; Bahrami, S.H. Application of heterogeneous nano-semiconductors for photocatalytic advanced oxidation of organic compounds: A review. *J. Environ. Chem. Eng.* **2019**, *7*, 103283. [CrossRef]
29. Almomani, F.; Rene, E.R.; Veiga, M.C.; Bhosale, R.R.; Kennes, C. Treatment of waste gas contaminated with dichloromethane using photocatalytic oxidation, biodegradation and their combinations. *J. Hazard. Mater.* **2021**, *405*, 123735. [CrossRef]
30. Mohseni, M.; Prieto, L. Biofiltration of hydrophobic VOCs pretreated with UV photolysis and photocatalysis. *Int. J. Environ. Technol. Manag.* **2008**, *9*, 47–58. [CrossRef]
31. Khezami, L.; Nguyen-Tri, P.; Saoud, W.A.; Bouzaza, A.; El Jery, A.; Duc Nguyen, D.; Gupta, V.K.; Assadi, A.A. Recent progress in air treatment with combined photocatalytic/plasma processes: A review. *J. Environ. Manag.* **2021**, *299*, 113588. [CrossRef]
32. Kuwahara, Y.; Yamashita, H. Efficient photocatalytic degradation of organics diluted in water and air using TiO_2 designed with zeolites and mesoporous silica materials. *J. Mater. Chem.* **2011**, *21*, 2407–2416. [CrossRef]
33. Baaloudj, O.; Nasrallah, N.; Bouallouche, R.; Kenfoud, H.; Khezami, L.; Assadi, A.A. High efficient Cefixime removal from water by the sillenite $Bi_{12}TiO_{20}$: Photocatalytic mechanism and degradation pathway. *J. Clean. Prod.* **2022**, *330*, 129934. [CrossRef]
34. Bolton, J.R.; Bircher, K.G.; Tumas, W.; Tolman, C.A. Figures-of-merit for the technical development and application of advanced oxidation technologies for both electric- and solar-driven systems. *Pure Appl. Chem.* **2001**, *73*, 627–637. [CrossRef]

35. Serhane, Y.; Belkessa, N.; Bouzaza, A.; Wolbert, D.; Assadi, A.A. Continuous air purification by front flow photocatalytic reactor: Modelling of the influence of mass transfer step under simulated real conditions. *Chemosphere* **2022**, *295*, 133809. [CrossRef] [PubMed]
36. Pelaez, M.; Nolan, N.T.; Pillai, S.C.; Seery, M.K.; Falaras, P.; Kontos, A.G.; Dunlop, P.S.M.; Hamilton, J.W.J.; Byrne, J.A.; O'Shea, K.; et al. A review on the visible light active titanium dioxide photocatalysts for environmental applications. *Appl. Catal. B Environ.* **2012**, *125*, 331–349. [CrossRef]
37. Kang, X.; Liu, S.; Dai, Z.; He, Y.; Song, X.; Tan, Z. Titanium dioxide: From engineering to applications. *Catalysts* **2019**, *9*, 191. [CrossRef]
38. Hodgson, A.T.; Destaillats, H.; Sullivan, D.P.; Fisk, W.J. Performance of ultraviolet photocatalytic oxidation for indoor air cleaning applications. *Indoor Air* **2007**, *17*, 305–316. [CrossRef]
39. Muscetta, M.; Russo, D. Photocatalytic applications in wastewater and air treatment: A patent review (2010–2020). *Catalysts* **2021**, *11*, 834. [CrossRef]
40. Riaz, N.; Fen, D.A.C.S.; Khan, M.S.; Naz, S.; Sarwar, R.; Farooq, U.; Bustam, M.A.; Batiha, G.E.S.; El Azab, I.H.; Uddin, J.; et al. Iron-zinc co-doped titania nanocomposite: Photocatalytic and photobiocidal potential in combination with molecular docking studies. *Catalysts* **2021**, *11*, 1112. [CrossRef]
41. Malliga, P.; Pandiarajan, J.; Prithivikumaran, N.; Neyvasagam, K. Effect of film thickness on structural and optical properties of TiO2 thin films. In Proceedings of the International Conference on Advanced Nanomaterials & Emerging Engineering Technologies, Chennai, India, 24–26 July 2013; Volume 2, pp. 488–491. [CrossRef]
42. Fagan, R.; McCormack, D.E.; Dionysiou, D.D.; Pillai, S.C. A review of solar and visible light active TiO_2 photocatalysis for treating bacteria, cyanotoxins and contaminants of emerging concern. *Mater. Sci. Semicond. Process.* **2016**, *42*, 2–14. [CrossRef]
43. Rabhi, S.; Belkacemi, H.; Bououdina, M.; Kerrami, A.; Ait Brahem, L.; Sakher, E. Effect of Ag doping of TiO_2 nanoparticles on anataserutile phase transformation and excellent photodegradation of amlodipine besylate. *Mater. Lett.* **2019**, *236*, 640–643. [CrossRef]
44. Yi, J.; Huang, L.; Wang, H.; Yu, H.; Peng, F. AgI/TiO_2 nanobelts monolithic catalyst with enhanced visible light photocatalytic activity. *J. Hazard. Mater.* **2015**, *284*, 207–214. [CrossRef]
45. Chen, Y.; Huang, W.; He, D.; Situ, Y.; Huang, H. Construction of heterostructured g-C_3N_4/Ag/TiO_2 microspheres with enhanced photocatalysis performance under visible-light irradiation. *ACS Appl. Mater. Interfaces* **2014**, *6*, 14405–14414. [CrossRef]
46. Monga, D.; Basu, S. Single-crystalline 2D BiOCl nanorods decorated with 2D MoS_2 nanosheets for visible light-driven photocatalytic detoxification of organic and inorganic pollutants. *FlatChem* **2021**, *28*, 100267. [CrossRef]
47. Guan, Z.; Li, Q.; Shen, B.; Bao, S.; Zhang, J.; Tian, B. Fabrication of Co_3O_4 and Au co-modified BiOBr flower-like microspheres with high photocatalytic efficiency for sulfadiazine degradation. *Sep. Purif. Technol.* **2020**, *234*, 116100. [CrossRef]
48. Raizada, P.; Thakur, P.; Sudhaik, A.; Singh, P.; Thakur, V.K.; Hosseini-Bandegharaei, A. Fabrication of dual Z-scheme photocatalyst via coupling of BiOBr/Ag/AgCl heterojunction with P and S co-doped g-C_3N_4 for efficient phenol degradation. *Arab. J. Chem.* **2020**, *13*, 4538–4552. [CrossRef]
49. Zhang, W.; Zhang, Q.; Dong, F. Visible-light photocatalytic removal of NO in air over BiOX (X = Cl, Br, I) single-crystal nanoplates prepared at room temperature. *Ind. Eng. Chem. Res.* **2013**, *52*, 6740–6746. [CrossRef]
50. Gao, F.; Yang, Y.; Wang, T. Preparation of porous TiO_2/Ag heterostructure films with enhanced photocatalytic activity. *Chem. Eng. J.* **2015**, *270*, 418–427. [CrossRef]
51. Xie, Z.; Yang, J.; Wang, K.; Meng, Q.; Tang, Y.; Zhao, K. Facile fabrication of TiO_2-SiO_2-C composite with anatase/rutile heterostructure via sol-gel process and its enhanced photocatalytic activity in the presence of H_2O_2. *Ceram. Int.* **2022**, *48*, 9114–9123. [CrossRef]
52. Eskandari, P.; Farhadian, M.; Solaimany Nazar, A.R.; Jeon, B.H. Adsorption and Photodegradation Efficiency of TiO_2/Fe_2O_3/PAC and TiO_2/Fe_2O_3/Zeolite Nanophotocatalysts for the Removal of Cyanide. *Ind. Eng. Chem. Res.* **2019**, *58*, 2099–2112. [CrossRef]
53. Pal, B.; Sharon, M.; Nogami, G. Preparation and characterization of TiO_2/Fe_2O_3 binary mixed oxides and its photocatalytic properties. *Mater. Chem. Phys.* **1999**, *59*, 254–261. [CrossRef]
54. Hou, F.; Lu, K.; Liu, F.; Xue, F.; Liu, M. Manipulating a TiO_2-graphene-Ta_3N_5 heterojunction for efficient Z-scheme photocatalytic pure water splitting. *Mater. Res. Bull.* **2022**, *150*, 111782. [CrossRef]
55. Li, H.; Hong, W.; Cui, Y.; Hu, X.; Fan, S.; Zhu, L. Enhancement of the visible light photocatalytic activity of Cu_2O/$BiVO_4$ catalysts synthesized by ultrasonic dispersion method at room temperature. *Mater. Sci. Eng. B* **2014**, *181*, 1–8. [CrossRef]
56. Aguilera-Ruiz, E.; García-Pérez, U.M.; De La Garza-Galván, M.; Zambrano-Robledo, P.; Bermúdez-Reyes, B.; Peral, J. Efficiency of Cu_2O/$BiVO_4$ particles prepared with a new soft procedure on the degradation of dyes under visible-light irradiation. *Appl. Surf. Sci.* **2015**, *328*, 361–367. [CrossRef]
57. Sun, S.; Ding, J.; Bao, J.; Gao, C.; Qi, Z.; Yang, X.; He, B.; Li, C. Photocatalytic degradation of gaseous toluene on Fe-TiO_2 under visible light irradiation: A study on the structure, activity and deactivation mechanism. *Appl. Surf. Sci.* **2012**, *258*, 5031–5037. [CrossRef]
58. Burda, C.; Lou, Y.; Chen, X.; Samia, A.C.S.; Stout, J.; Gole, J.L. Enhanced nitrogen doping in TiO_2 nanoparticles. *Nano Lett.* **2003**, *3*, 1049–1051. [CrossRef]
59. Hua, L.; Yin, Z.; Cao, S. Recent advances in synthesis and applications of carbon-doped TiO_2 nanomaterials. *Catalysts* **2020**, *10*, 1431. [CrossRef]

60. Hanaor, D.A.H.; Sorrell, C.C. Review of the anatase to rutile phase transformation. *J. Mater. Sci.* **2011**, *46*, 855–874. [CrossRef]
61. Ghumro, S.S.; Lal, B.; Pirzada, T. Visible-Light-Driven Carbon-Doped TiO_2-Based Nanocatalysts for Enhanced Activity toward Microbes and Removal of Dye. *ACS Omega* **2022**, *7*, 4333–4341. [CrossRef]
62. Akhter, P.; Arshad, A.; Saleem, A.; Hussain, M. Recent Development in Non-Metal-Doped Titanium Dioxide Photocatalysts for Different Dyes Degradation and the Study of Their Strategic Factors: A Review. *Catalysts* **2022**, *12*, 1331. [CrossRef]
63. Zhang, W.; Luo, N.; Huang, S.; Wu, N.L.; Wei, M. Sulfur-Doped Anatase TiO_2 as an Anode for High-Performance Sodium-Ion Batteries. *ACS Appl. Energy Mater.* **2019**, *2*, 3791–3797. [CrossRef]
64. Niu, P.; Wu, G.; Chen, P.; Zheng, H.; Cao, Q.; Jiang, H. Optimization of Boron Doped TiO_2 as an Efficient Visible Light-Driven Photocatalyst for Organic Dye Degradation With High Reusability. *Front. Chem.* **2020**, *8*, 172. [CrossRef]
65. Piątkowska, A.; Janus, M.; Szymański, K.; Mozia, S. C-, N- and S-doped TiO_2 photocatalysts: A review. *Catalysts* **2021**, *11*, 144. [CrossRef]
66. Marschall, R. Semiconductor composites: Strategies for enhancing charge carrier separation to improve photocatalytic activity. *Adv. Funct. Mater.* **2014**, *24*, 2421–2440. [CrossRef]
67. Jones, A.P. Indoor air quality and health. *Atmos. Environ.* **1999**, *33*, 4535–4564. [CrossRef]
68. Magureanu, M.; Bogdan, N.; Hu, J.; Richards, R.; Florea, M.; Parvulescu, M. Plasma-assisted catalysis total oxidation of trichloroethylene over gold nano-particles embedded in SBA-15 catalysts. *Catal. B Environ.* **2007**, *76*, 275–281. [CrossRef]
69. Xia, Y.; Xia, L.; Liu, Y.; Yang, T.; Deng, J.; Dai, H. Concurrent catalytic removal of typical volatile organic compound mixtures over Au-Pd/α-MnO_2 nanotubes. *J. Environ. Sci.* **2018**, *64*, 276–288. [CrossRef] [PubMed]
70. Bahri, M.; Haghighat, F. Plasma-based indoor air cleaning technologies: The state of the art-review. *Clean Soil Air Water* **2014**, *42*, 1667–1680. [CrossRef]
71. Shah, K.W.; Li, W. A review on catalytic nanomaterials for volatile organic compounds VOC removal and their applications for healthy buildings. *Nanomaterials* **2019**, *9*, 910. [CrossRef]
72. Tobaldi, D.M.; Dvoranová, D.; Lajaunie, L.; Rozman, N.; Figueiredo, B.; Seabra, M.P.; Škapin, A.S.; Calvino, J.J.; Brezová, V.; Labrincha, J.A. Graphene-TiO_2 hybrids for photocatalytic aided removal of VOCs and nitrogen oxides from outdoor environment. *Chem. Eng. J.* **2021**, *405*. [CrossRef]
73. Lam, S.M.; Sin, J.C.; Abdullah, A.Z.; Mohamed, A.R. Photocatalytic TiO_2/carbon nanotube nanocomposites for environmental applications: An overview and recent developments. *Fuller. Nanotub. Carbon Nanostruct.* **2014**, *22*, 471–509. [CrossRef]
74. Shayegan, Z.; Lee, C.S.; Haghighat, F. TiO_2 photocatalyst for removal of volatile organic compounds in gas phase—A review. *Chem. Eng. J.* **2018**, *334*, 2408–2439. [CrossRef]
75. Zadi, T.; Azizi, M.; Nasrallah, N.; Bouzaza, A.; Zadi, T.; Azizi, M.; Nasrallah, N.; Bouzaza, A.; Maachi, R. Indoor air treatment of refrigerated food chambers with synergetic association between cold plasma and photocatalysis: Process performance and photocatalytic poisoning. *Chem. Eng. J.* **2020**, *382*, 122951. [CrossRef]
76. Abou Saoud, W.; Kane, A.; Le Cann, P.; Gerard, A.; Lamaa, L.; Peruchon, L.; Brochier, C.; Bouzaza, A.; Wolbert, D.; Assadi, A.A. Innovative photocatalytic reactor for the degradation of VOCs and microorganism under simulated indoor air conditions: Cu-Ag/TiO_2-based optical fibers at a pilot scale. *Chem. Eng. J.* **2021**, *411*, 128622. [CrossRef]
77. Jia, Z.; Barakat, C.; Dong, B.; Rousseau, A. VOCs Destruction by Plasma Catalyst Coupling Using AL-KO PURE Air Purifier on Industrial Scale. *J. Mater. Sci. Chem. Eng.* **2015**, *3*, 19–26. [CrossRef]
78. Abidi, M.; Hajjaji, A.; Bouzaza, A.; Trablesi, K.; Makhlouf, H.; Rtimi, S.; Assadi, A.A.; Bessais, B. Simultaneous removal of bacteria and volatile organic compounds on Cu_2O-NPs decorated TiO_2 nanotubes: Competition effect and kinetic studies. *J. Photochem. Photobiol. A Chem.* **2020**, *400*, 112722. [CrossRef]
79. Vincent, G.; Queffeulou, A.; Marquaire, P.M.; Zahraa, O. Remediation of olfactory pollution by photocatalytic degradation process: Study of methyl ethyl ketone (MEK). *J. Photochem. Photobiol. A Chem.* **2007**, *191*, 42–50. [CrossRef]
80. Vincent, G.; Schaer, E.; Marquaire, P.M.; Zahraa, O. CFD modelling of an annular reactor, application to the photocatalytic degradation of acetone. *Process Saf. Environ. Prot.* **2011**, *89*, 35–40. [CrossRef]
81. Liu, H.; Li, C.; Ren, X.; Liu, K.; Yang, J. Fine platinum nanoparticles supported on a porous ceramic membrane as efficient catalysts for the removal of benzene. *Sci. Rep.* **2017**, *7*, 16589. [CrossRef]
82. Sedjame, H.J.; Fontaine, C.; Lafaye, G.; Barbier, J. On the promoting effect of the addition of ceria to platinum based alumina catalysts for VOCs oxidation. *Appl. Catal. B Environ.* **2014**, *144*, 233–242. [CrossRef]
83. Xu, Z.; Yu, J.; Jaroniec, M. Efficient catalytic removal of formaldehyde at room temperature using AlOOH nanoflakes with deposited Pt. *Appl. Catal. B Environ.* **2015**, *163*, 306–312. [CrossRef]
84. Zhang, J.; Li, Y.; Wang, L.; Zhang, C.; He, H. Catalytic oxidation of formaldehyde over manganese oxides with different crystal structures. *Catal. Sci. Technol.* **2015**, *5*, 2305–2313. [CrossRef]
85. Zhang, C.; He, H.; Tanaka, K. ichi Catalytic performance and mechanism of a Pt/TiO_2 catalyst for the oxidation of formaldehyde at room temperature. *Appl. Catal. B Environ.* **2006**, *65*, 37–43. [CrossRef]
86. Kucherov, A.V.; Tkachenko, O.P.; Kirichenko, O.A.; Kapustin, G.I.; Mishin, I.V.; Klementiev, K.V.; Ojala, S.; Kustov, L.M.; Keiski, R. Nanogold-containing catalysts for low-temperature removal of S-VOC from air. *Top. Catal.* **2009**, *52*, 351–358. [CrossRef]
87. Assadi, A.A.; Bouzaza, A.; Vallet, C.; Wolbert, D. Use of DBD plasma, photocatalysis, and combined DBD plasma/photocatalysis in a continuous annular reactor for isovaleraldehyde elimination—Synergetic effect and byproducts identification. *Chem. Eng. J.* **2014**, *254*, 124–132. [CrossRef]

88. Chen, C.Y.; Wu, L.C.; Chen, H.Y.; Chung, Y.C. Inactivation of *Staphylococcus aureus* and *Escherichia coli* in water using photocatalysis with fixed TiO_2. *Water. Air Soil Pollut.* **2010**, *212*, 231–238. [CrossRef]
89. Blanco-Galvez, J.; Fernández-Ibáñez, P.; Malato-Rodríguez, S. Solar photo catalytic detoxification and disinfection of water: Recent overview. *J. Sol. Energy Eng. Trans. ASME* **2007**, *129*, 4–15. [CrossRef]
90. Magaña-López, R.; Zaragoza-Sánchez, P.I.; Jiménez-Cisneros, B.E.; Chávez-Mejía, A.C. The use of TiO_2 as a disinfectant in water sanitation applications. *Water* **2021**, *13*, 1641. [CrossRef]
91. Anucha, C.B.; Altin, I.; Bacaksiz, E.; Stathopoulos, V.N. Titanium dioxide (TiO_2)-based photocatalyst materials activity enhancement for contaminants of emerging concern (CECs) degradation: In the light of modification strategies. *Chem. Eng. J. Adv.* **2022**, *10*, 100262. [CrossRef]
92. Rtimi, S.; Dionysiou, D.D.; Pillai, S.C.; Kiwi, J. Advances in catalytic/photocatalytic bacterial inactivation by nano Ag and Cu coated surfaces and medical devices. *Appl. Catal. B Environ.* **2019**, *240*, 291–318. [CrossRef]
93. Saoud, W.A.; Assadi, A.A.; Kane, A.; Jung, A.; Cann, P.L.; Bazantay, F.; Bouzaza, A.; Wolbert, D. Integrated process for the removal of indoor VOCs from food industry manufacturing Elimination of Butane-2,3-dione and Heptan-2-one by cold plasma-photocatalysis combination. *Photochem. Photobiol. A Chem.* **2020**, *386*, 112071. [CrossRef]
94. Venieri, D.; Gounaki, I.; Bikouvaraki, M.; Binas, V.; Zachopoulos, A.; Kiriakidis, G.; Mantzavinos, D. Solar photocatalysis as disinfection technique: Inactivation of *Klebsiella pneumoniae* in sewage and investigation of changes in antibiotic resistance profile. *J. Environ. Manag.* **2017**, *195*, 140–147. [CrossRef]
95. Ray, S.K.; Dhakal, D.; Regmi, C.; Yamaguchui, T.; Lee, S.W. Inactivation of *Staphylococcus aureus* in visible light by morphology tuned α-$NiMoO_4$. *J. Photochem. Photobiol. A Chem.* **2018**, *350*, 59–68. [CrossRef]
96. Kőrösi, L.; Pertics, B.; Schneider, G.; Bognár, B.; Kovács, J.; Meynen, V.; Scarpellini, A.; Pasquale, L.; Prato, M. Photocatalytic inactivation of plant pathogenic bacteria using TiO_2 nanoparticles prepared hydrothermally. *Nanomaterials* **2020**, *10*, 1730. [CrossRef] [PubMed]
97. Salavati-Niasari, M.; Davar, F. Synthesis of copper and copper(I) oxide nanoparticles by thermal decomposition of a new precursor. *Mater. Lett.* **2009**, *63*, 441–443. [CrossRef]
98. Yue, Y.; Zhang, P.; Wang, W.; Cai, Y.; Tan, F.; Wang, X.; Qiao, X.; Wong, P.K. Enhanced dark adsorption and visible-light-driven photocatalytic properties of narrower-band-gap Cu_2S decorated Cu_2O nanocomposites for efficient removal of organic pollutants. *J. Hazard. Mater.* **2020**, *384*, 121302. [CrossRef] [PubMed]
99. Wang, W.; Song, J.; Kang, Y.; Chai, D.; Zhao, R.; Lei, Z. Sm_2O_3 embedded in nitrogen doped carbon with mosaic structure: An effective catalyst for oxygen reduction reaction. *Energy* **2017**, *133*, 115–120. [CrossRef]
100. Gupta, S.B.; Bluhm, H. The potential of pulsed underwater streamer discharges as a disinfection technique. *IEEE Trans. Plasma Sci.* **2008**, *36*, 1621–1632. [CrossRef]
101. Tijani, J.O.; Fatoba, O.O.; Madzivire, G.; Petrik, L.F. A review of combined advanced oxidation technologies for the removal of organic pollutants from water. *Water Air Soil Pollut.* **2014**, *225*, 2102. [CrossRef]
102. Ado, A.; Tukur, A.I.; Ladan, M.; Gumel, S.M.; Muhammad, A.A.; Habibu, S.; Koki, I.B. A Review on Industrial Effluents as Major Sources of Water Pollution in Nigeria. *Chem. J.* **2015**, *1*, 159–164.
103. Weiss, C.; Carriere, M.; Fusco, L.; Fusco, L.; Capua, I.; Regla-Nava, J.A.; Pasquali, M.; Pasquali, M.; Pasquali, M.; Scott, J.A.; et al. Toward Nanotechnology-Enabled Approaches against the COVID-19 Pandemic. *ACS Nano* **2020**, *14*, 6383–6406. [CrossRef] [PubMed]
104. Karbasi, M.; Karimzadeh, F.; Raeissi, K.; Rtimi, S.; Kiwi, J.; Giannakis, S.; Pulgarin, C. Insights into the photocatalytic bacterial inactivation by flower-like Bi_2WO_6 under solar or visible light, through in situ monitoring and determination of reactive oxygen species (ROS). *Water* **2020**, *12*, 1099. [CrossRef]
105. Singh, J.; Juneja, S.; Palsaniya, S.; Manna, A.K.; Soni, R.K.; Bhattacharya, J. Evidence of oxygen defects mediated enhanced photocatalytic and antibacterial performance of ZnO nanorods. *Colloids Surf. B Biointerfaces* **2019**, *184*, 110541. [CrossRef]
106. Wang, W.; Wang, H.; Li, G.; An, T.; Zhao, H.; Wong, P.K. Catalyst-free activation of persulfate by visible light for water disinfection: Efficiency and mechanisms. *Water Res.* **2019**, *157*, 106–118. [CrossRef]
107. Hajjaji, A.; Elabidi, M.; Trabelsi, K.; Assadi, A.A.; Bessais, B.; Rtimi, S. Bacterial adhesion and inactivation on Ag decorated TiO_2-nanotubes under visible light: Effect of the nanotubes geometry on the photocatalytic activity. *Colloids Surf. B Biointerfaces* **2018**, *170*, 92–98. [CrossRef] [PubMed]
108. Ubonchonlakate, K.; Sikong, L.; Saito, F. Photocatalytic disinfection of *P. aeruginosa* bacterial Ag-doped TiO_2 film. *Procedia Eng.* **2012**, *32*, 656–662. [CrossRef]
109. Lee, M.; Shahbaz, H.M.; Kim, J.U.; Lee, H.; Lee, D.U.; Park, J. Efficacy of UV-TiO_2 photocatalysis technology for inactivation of *Escherichia coli* K12 on the surface of blueberries and a model agar matrix and the influence of surface characteristics. *Food Microbiol.* **2018**, *76*, 526–532. [CrossRef] [PubMed]

110. Gupta, K.; Singh, R.P.; Pandey, A.; Pandey, A. Photocatalytic antibacterial performance of TiO_2 and Ag-doped TiO_2 against *S. aureus*, *P. aeruginosa* and *E. coli*. *Beilstein J. Nanotechnol.* **2013**, *4*, 345–351. [CrossRef] [PubMed]
111. Guzman, M.; Dille, J.; Godet, S. Synthesis and antibacterial activity of silver nanoparticles against gram-positive and gram-negative bacteria. *Nanomed. Nanotechnol. Biol. Med.* **2012**, *8*, 37–45. [CrossRef] [PubMed]